Eur. Phys. J. Plus (2018) **133**: 405
DOI 10.1140/epjp/i2018-12201-1

THE EUROPEAN PHYSICAL JOURNAL PLUS

Regular Article

The design of a vibration control system for an aluminum plate with piezo-stripes based on residues analysis of model

Andrzej Koszewnik[a]

Bialystok University of Technology, Faculty of Mechanical Engineering, Department of Automatics and Robotics, Wiejska 45C, 15-351 Bialystok, Poland

Received: 23 November 2017 / Revised: 30 July 2018
Published online: 5 October 2018

Abstract. The design process of an active vibration control system for many mechanical structures using smart devices requires determining reduced and precise mathematical models. Such requirements cause orthogonal methods to be used and carefully analyzed. In the present paper, a plate with two simple supported edges and two free edges (SFSF) is an object of consideration. It is known that this structure represents a flexible structure wherein high natural frequencies are separated from low frequencies because they are naturally damped. Thus, in order to estimate the dynamical features of the control system, some orthogonal methods, such as the Schur and modal decomposition, were applied. A detailed analysis of the chosen methods showed us that each of them properly generates resonance frequencies while calculating different values of the anti-resonance frequencies. From the strategy control point of view, it is known that the anti-resonances play an essential role because they directly influence the dynamics of the whole control system. Thus, in order to check this behavior, different controllers are designed for various reduced models and, next, they are applied in a real mechanical structure. The dynamical behavior of the control systems with such controllers was analyzed and tested on a laboratory stand. In conclusion, we should carefully choose model reduction methods in the design process of the vibration control system. The sum of the residues of the reduced model appeared to be the best indicator during the choice process of the reduction method. It is particularly important when we design the vibration control system for a non-existent yet, but newly designed, structure.

Introduction

The increase of dimensions and reduction of masses of mechanical structures lead to their higher flexibility and compliance to internal and external excitations. Therefore, active vibration control systems of flexible structures gain more and more popularity. The reduction of the mathematical models of the structure is an important problem in the case when the vibration control system using smart devices is being designed. The model reduction simplifies this procedure but makes some features of the real control system more uncertain. With the reduction of the flexible structure models the following problems appear: optimal location of sensors and actuators [1], "spillover" of the measurement and control effects on the rejected part of the model [2], insufficient frequency bandwidth of the sensors and actuators [3], unknown damping components of the structure [4], sensor/actuator non-collocation [5,6].

When the control system is applied to the existing stable structure, some of the problems can be facilitated by the identification procedures. For the known damped modes, the observability and the observability Gramians are used to design the control system [7]. In this case, the Hankel Singular Values [8] indicate the sensitive modes which can be measured and controlled, and separate them from the rejected part of the system. Finally, the control law is determined according to a chosen method [6].

For the non-existent but newly designed flexible structures, the FEM (Finite Element Method) is used to predict the strength and dynamical properties of a real plant. Such approach is used to describe the vibrations in such applications as: active tendons [9], flexible rotors [10,11], flexible gyroscopic systems [12], spacecrafts [13], trusses [14] or beams [15]. The structure mass and flexibility matrices are well calculated by available computer procedures which allows deriving simple dynamic equations of motion without elements connected with damping. The eigenproblem

[a] e-mail: a.koszewnik@pb.edu.pl

(natural frequencies, mode shapes) can be estimated and solved on the basis of such a model. The model with many eigenvectors and eigenvalues is helpful in describing the dynamic behavior of the investigated structures. However, from the strategy control point of view it is still difficult to generate a proper control law. Thus, in order to simplify this problem, the model with a large number of elastic coordinates (in Cartesian space) should be reduced according to known orthogonal methods [6,16].

The modal decomposition is the first classical method for the linear model reduction. According to this method, the eigenvectors and eigenvalues are used to separate the dynamics of the particular modes and the modes are divided into controlled and non-controlled modes. Apart from the aforementioned modal method, the Gyuan reduction [6], Rayleigh-Ritz method [17] or Schur decomposition [16] are used to describe the vibration of structures (beams or bar structures). In all reduction methods the eigenvalue problem of the considered structure is solved by the determination of approximation functions of the mode shapes and natural frequencies based on the assumed boundary and initial conditions.

The actuators include: magnetoreological dampers [18], magnetic bearings [19], piezoelectric actuators [20], electrohydraulic devices [21], which have a wide bandwidth and play an important role in such systems. In recent years the mentioned piezoelectric devices have become a strong group among modern smart actuators/sensors. For this reason, in some cases there is a need to use special control techniques to ensure a proper control system. Then, not only the control law is designed, but also a proper location and orientation of the sensors and actuators on the structure are optimized [22–24].

Taking into account the piezoelectric actuators and the type of structure, the influence of the aforementioned orthogonal methods on the dynamics of the whole system was analyzed for a 1D structure for the purpose of this paper [25]. The investigations carried out for a cantilever beam with a non-collocated pair of an actuator and a sensor showed that all the considered orthogonal methods properly generated natural frequencies while calculating different values of anti-resonance frequencies. This caused a need to check how those anti-resonance frequencies influence the stability of the mechanical structure. As a result, the boundary gains of the feedback loop for each reduced order model written in a partial-fraction form have been determined and compared with each other.

In the present paper, the problem of the orthogonal methods influence on the dynamics of the system is analyzed once again for a 2D mechanical structure as the development of the research described in [25]. The control plant in this case is the SFSF plate with non-collocated two-pair piezo-elements (sensor, actuator). The numerical investigations carried out for this structure and described in paper [26] showed that the choice of proper locations and orientations of piezo-elements for this type of structure is a crucial stage in the design procedure of a vibration control system. It is especially important when designing a control system for rectangular 2D smart structures in which the applied piezo-stripes generate extensions only in longitudinal directions. Therefore, taking into account the mode shapes of this structure and the behavior of the piezo-element, the whole TITO control system can be decoupled into two SISO subsystems. The subsystems obtained in this way, which describe vibrations of the plate in two perpendicular directions X (analysis of odd modes) and Y (even modes), allow determining open-loop reduced order models by using the considered orthogonal methods. Then, for each model written in the partial-fraction form, the boundary of their stability can be found with the use of the root-locus method. Finally, the gains of the controller, obtained as a result of the simulation investigations, are applied to test the closed-loop subsystem with the full order model.

The obtained simulation and experimental results have shown a strong correlation between gains of the proportional controller and the sum of residues of the open-loop reduced model.

Mathematical modelling of the smart plate

The aluminum plate with SFSF boundary conditions and also with piezo-actuators and piezo-sensors, shown in fig. 1, is an object of consideration. The piezo-elements A-1 and A-2 located on top of the plate work as actuators, but elements S-1 and S-2, located on the opposite site and denoted by the dash line, work as sensors. The parameters of this structure and piezo-patches used in the system are collected in table 1. The whole process of determining the orientation and locations of these piezo-elements for this structure is described in detail in [26]. Such an approach to the modelling of this type of mechanical structures allows considering two independent control systems for separately controlling the chosen modes (even or odd) in the frequency range of 10–250 Hz.

General model of the mechanical structure

In the modern approach, the vibration properties of many mechanical structures are analyzed based on the appropriate software which uses a numerical model. In most cases such a model is determined with the use of a well-known from literature Finite Element Method (FEM) that allows to discretize a chosen mechanical structure into many small elements called finite elements. For such determined elements the stiffness and mass matrices are calculated and then

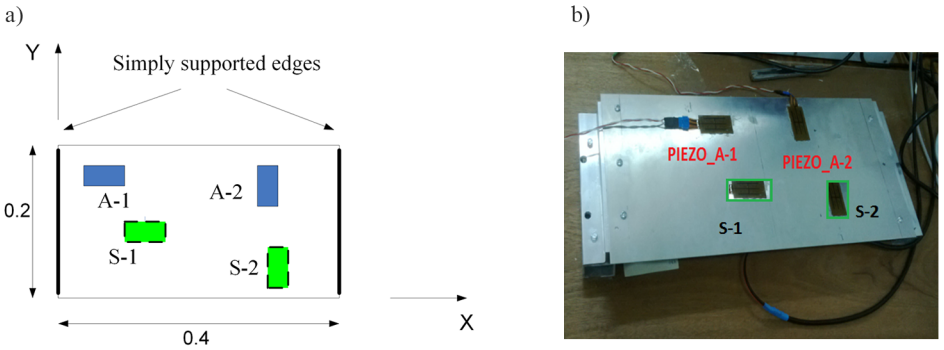

Fig. 1. The SFSF plate with piezo-actuators and piezo-sensors: (a) model of the SFSF plate with piezo-patches located at their quasi-optimal locations; (b) photo of the plate located on the lab stand.

Table 1. The parameters of the plate and the used piezo-elements.

Parameter	Plate		Piezo-element	Actuator QP20N	Sensor QP10N
Length [m]	l	0.4	l_p	0.05	0.05
Width [m]	B	0.2	b_p	0.025	0.025
Thickness [m]	h	0.002	h_a/h_s	0.000782	0.000357
Young module [GPa]	E_b	200	E_p	0.18	0.18
Density [kg/m^3]	ρ_b	7800	ρ_p	7200	7200
Piezoelectric strain constant [m/V]	–	–	d_{31}	$-125\text{e}-12$	–
Piezoelectric stress/charge constant [C/m^2]	–	–	e_{31}	–	-7.5

connected with other elements by considering a proper number of nodes and boundary conditions. As a result the global stiffness $\mathbf{K}$ and mass $\mathbf{M}$ matrices are calculated. Matrices obtained in this way allow to determine the mathematical model of the mechanical structure described in eq. (1) and next to derive the undamped resonance frequencies ω_i $(i = 1, 2, 3, 4, \ldots)$ and undamped mode shapes φ_i $(i = 1, 2, 3, 4, \ldots)$,

$$\mathbf{M}\ddot{\mathbf{x}} + \mathbf{K}\mathbf{x} = \mathbf{0}. \tag{1}$$

Next, taking into account [27] each SISO subsystem mentioned in the Introduction with non-collocated piezo-stripes (sensor/actuator) can be expressed in the form of a partial fraction description in the following form:

$$G(s) = \sum_{i=1}^{n\to\infty} \frac{1}{m_i}\left(\frac{\phi_i(k)\phi_i(l)}{(s^2+\omega_i^2)}\right) = \frac{1}{m_i}\cdot\frac{\phi_i(k)\phi_i(l)}{(s^2+\omega_i^2)} = \frac{1}{m_i}\left(\frac{R_{i1}}{s+j\omega_i} + \frac{R_{i2}}{s-j\omega_i}\right), \tag{2}$$

where m_i is the i-th modal mass, ω_i is the i-th natural frequency, $\varphi_i(k)$, $\varphi_i(l)$ are the modal amplitudes of the actuator and the sensor at the points k, l, respectively, $\pm j\omega_i$ are the poles of the transfer function, R_{i1}, R_{i2} are the residues of the following values

$$R_{i1} = \frac{j\varphi_i(k)\varphi_i(l)}{2\omega_i}, \qquad R_{i2} = \frac{-j\varphi_i(k)\varphi_i(l)}{2\omega_i}. \tag{3}$$

In the case of considering the damped system, each element of the transfer function can be express in the following form:

$$\frac{\varphi_i(k)\varphi_i(l)}{(s^2+2\alpha_i s+\alpha_i^2+\omega_i^2)} = \frac{R_{i1}}{s+\alpha_i+j\omega_i} + \frac{R_{i2}}{s+\alpha_i-j\omega_i}, \tag{4}$$

where $\alpha_i \pm j\omega_i$ are the real and imaginary parts of the poles of the transfer function, respectively, and R_{i1}, R_{i2} are the residues of the same form as in eq. (3).

Taking into account eqs. (2) to (4), we can see that the sum of residues always equals zero for any mode. This means that the sum of all residues in the whole model (eq. (2)) also equals zero,

$$R_{11} + R_{12} + R_{21} + R_{22} + R_{31} + R_{32} + \ldots = 0. \tag{5}$$

Moreover, the sum does not depend on the damping or location of the sensor and actuator. Intuitively, the reduction method which generates the model with the smallest sum of residues will be more convenient for the control system

purposes. Therefore, in the paper, it will be checked if the sum of residues can be used as an indicator of the best method of the model reduction.

The model in eq. (2) is rewritten as a zero-pole transfer function form [27]

$$G(s) = k\frac{\prod_{\text{zeros}}(s+\omega_{oi}^2)}{\prod_{\text{poles}}(s+\omega_i^2)}\,, \tag{6}$$

where ω_{oi} is the i-th anti-resonance frequency.

The model of the system presented in eq. (6) is useful in the design process of a control law for flexible structures. For systems where poles and zeros interlace, theoretically, the gain value in the feedback loop is infinite and the full closed loop system is still on the stability boundary [27]. This suggests that the stability boundary of the reduced system is correlated with the sum of residues and this correlation will be analyzed in the present paper. In the process of model reduction usually the high frequency poles and zeros are rejected but some additional actions are undertaken to keep the dynamical characteristics as close as possible to the real plant. The additional action causes changes of low-frequency characteristics of the reduced model by the changes of: only poles, only zeros or zeros and poles.

For example, in the Guyan method of model reductions [6], the poles and zeros are modified. It is safer and simpler to control the orthogonal models and the orthogonality is connected with poles. Therefore, in this investigations the reduction methods which influence the zeros of the transfer function is considered. A few methods will be investigated, namely: modal and Schur decompositions.

To find the stability boundary of the closed-loop subsystem with a proportional controller, the root locus method will be used. For each considered orthogonal methods the model of the plate is expressed in the following form:

$$G(s) = \sum_{i=1}^{N}\frac{\varphi_i(k)\varphi_i(l)}{m_i\,(s^2+2\alpha_i s+\alpha_i^2+\omega_i^2)} + R_0 = \sum_{i=1}^{N}\frac{1}{m_i}\frac{R_{i1}}{(s+\alpha_i+j\omega_i)} + \sum_{i=1}^{N}\frac{1}{m_i}\frac{R_{i2}}{(s+\alpha_i-j\omega_i)} + R_0, \tag{7}$$

where N is the considered amount of mode shapes, R_{i1}, R_{i2} are the residues of the transfer function for i-th mode shape, R_0 is the static residue.

The static residuum R_0 in eq. (7) influences the system dynamics, makes the plant non-strictly proper, increases the number of anti-resonance frequencies, and participates in the sum of residues.

Identification procedure of the plate parameters

The parameter identification procedure of a structure in this way was the first step of investigations that allowed examining the impact of orthogonal methods on correctness of the obtained reduced order model. For this reason, the smart plate was excited to vibrations by applying the applied chirp signal to one of the piezo-actuators A-1 or A-2 located on top of the surface. The frequency of the excitation signal was set in the range of 10–250 Hz, which contains the first three odd modes and the first two even modes. During the experiment, the amplitude of vibrations of the plate was also measured by the sensor element S-1 or S-2. Those measurements lead to obtain two frequency response functions (A-1–S-1) and (A-2–S-2), shown in fig. 2.

As can be seen in fig. 2, the location of the sensor plays an important role in the process of designing the control law. From the strategy control point of view the location of the sensors is a crucial issue for rectangular membranes or plates, because, when used in an experiment, piezo-stripes generate elongations only in longitudinal directions. This leads to obtain two non-collocated control subsystems. The analysis of fig. 2 shows that the vibration amplitude can be a good indicator when designing the control law because it influences to obtain a low-energy control system. It is especially visible in the range of frequencies between 60–70 Hz where the amplitude peak of vibration was only measured by the S-2 piezo. This also leads to distinguishing two subsystems, each of them describing only odd or even modes, respectively. As a result the first subsystem, further called "odd modes", represents the lowest three odd mode shapes (grey dotted line), but the other subsystem, called "even modes" (dot black line), represents the vibration of the plate only for the two lowest even mode shapes.

Next, taking into account the auto-regressive model and the reduction order process described in detail in the reference [26], the reduced order models of particular sub-systems are obtained and expressed in the following forms, respectively:

$$G_{\text{odd}}(s) = \frac{Y_{\text{odd}}(s)}{U(s)} = 0.0168\cdot\frac{(s^2+11.23s+6.482e4)(s^2+46.47s+9.353e5)(s^2+62.66s+2.685e6)}{(s^2+7.641s+4.885e4)(s^2+36.7s+8.443e5)(s^2+50.08s+2.574e6)}\,, \tag{8}$$

$$G_{\text{even}}(s) = \frac{Y_{\text{even}}(s)}{U(s)} = -0.00142\cdot\frac{(s^2+6.32s+3.273e5)(s^2+25.98s+1.403e6)}{(s^2+22.84s+1.896e5)(s^2+60.88s+9.953e5)}\,. \tag{9}$$

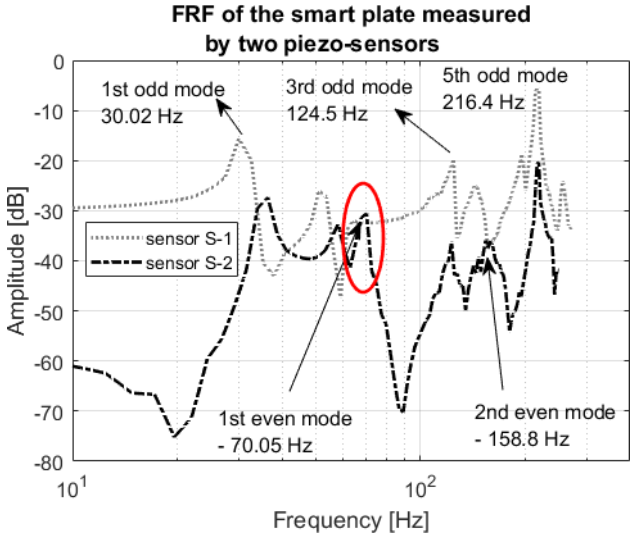

Fig. 2. The FRF of the SFSF smart plate obtained for the piezo-stripe sensor oriented longitudinally to X axis (S-1) and longitudinally to Y axis (S-2).

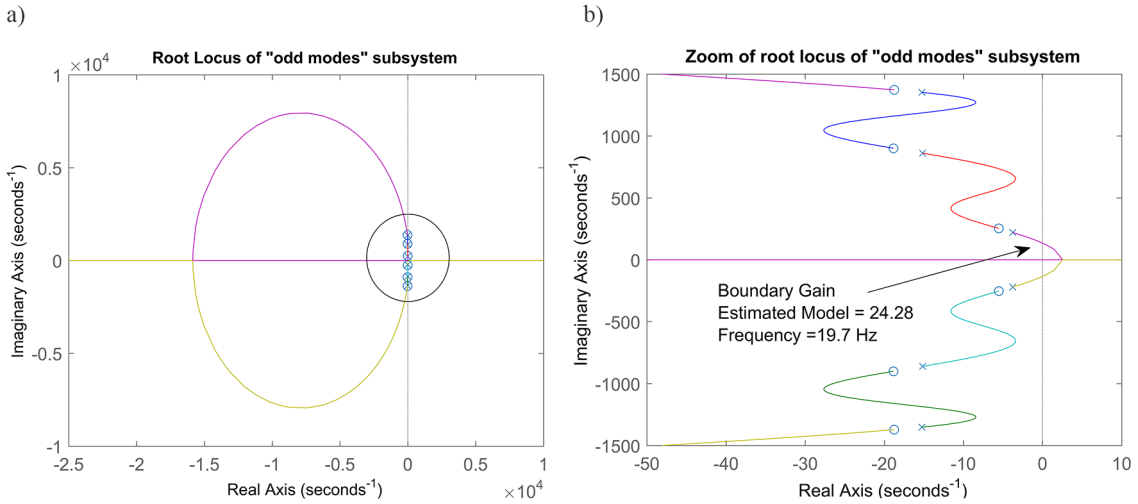

Fig. 3. The Evans plot for the estimated model obtained from experimental identification.

As a result, models estimated in this way for residue analysis are transformed to the partial-fraction form. Then, each model from eqs. (8) and (9) is expressed in the following form, respectively:

$$G_{\text{odd}}(s) = \frac{-0.005 + 0.9722j}{s-(-3.8-188.71j)} + \frac{-0.005 + 0.9722j}{s-(-3.8+188.71j)} + \frac{-0.0926 + 0.9984j}{s-(-18.4-781.6j)} + \frac{-0.0926 - 0.9984j}{s-(-18.4-781.6j)} + \frac{-0.0728 + 0.4635j}{s-(-25+1362.8j)} + \frac{-0.0728 - 0.4635j}{s-(-25+1362.8j)} - 0.0241, \tag{10}$$

$$G_{\text{even}}(s) = \frac{0.0077 + 0.243j}{s-(-30.4-997.2j)} + \frac{0.0077 - 0.243j}{s-(-30.4+997.2j)} + \frac{0.0378 + 0.339j}{s-(-11.4-435.2j)} + \frac{0.0378 - 0.339j}{s-(-11.4-435.2j)} - 0.0014. \tag{11}$$

The residue analysis of models expressed in eqs. (10) and (11) shows that the sum of particular models equals -0.4308 for "odd modes" and -0.0987 for "even modes", respectively. The calculated values become the basis for designing a proper vibration control system by using the root-locus method. The gains of the controllers, determined in this way, are boundary gains, which ensure stability of the whole control system. Firstly, the "odd modes" system is investigated. For this model, with the help of the Evans plot, such a boundary gain is determined and the results of this procedure are shown in fig. 3.

The analysis of the obtained plots shows that the designed control system is unstable. Evidently, it is visible in the case of two branches which are plotted on the right half-plane of the Evans plot. Then, in order to ensure the stability of the estimated model, the gain of the proportional controller in the feedback loop should not exceed the value of 24.28.

Influence of the reduction order methods to the value of the boundary gain

In further investigations we need to check how the choice of the reduction order methods influence the value of the residue sum of the reduced order model and the boundary gain determined with the help of the Evans plot. Firstly, the modal analytical method was chosen. Taking into account ref. [28] and a chosen method, the differential equation of a plate in geometric variables takes the following form:

$$D\Delta^2 z(x,y) = D\left(\frac{\partial^4 z(x,y)}{\partial x^4} + 2\frac{\partial^4 z(x,y)}{\partial x^2 \partial y^2} + \frac{\partial^4 z(x,y)}{\partial y^4}\right) = 0, \tag{12}$$

where D is the flexural rigidity of the considered plate, z is the vertical displacement of the plate.

The considered plate with simply supported short edges parallel to the Y-axis was already considered in [26]. Thus, taking into account the boundary conditions from the reference [26] the vertical deflection of the plate can be expressed in the following form:

$$z(x,y) = \sum_{n=1}^{5} \left(A_i \cosh(\alpha_i y) + B_i \sinh(\alpha_i y) + C_i \alpha_i \cosh(\alpha_i y) + D_i \alpha_i \sinh(\alpha_i y)\right) \sin \alpha_i x, \tag{13}$$

where $\alpha_i = \frac{i\pi}{l}$, i is the i-th mode shape, A_i, B_i, C_i, D_i are the coefficients of the vertical deflection determined individually for each mode shape.

Coefficients obtained in this way, put in eq. (13), allowdrawing the first five mode shapes of the plate, which is shown in fig. 4.

As it is known from the reference [26], the considered plate has two piezo-actuators: A-1 and A-2, and two piezo-sensors: S-1 and S-2 which are located in the quasi-optimal locations. The indicated locations and orientations of actuators lead to generate two bending moments $M_x(x,y)$ and $M_y(x,y)$ in the X- and Y-directions and obtain the total unit elongations of the structure in two perpendicular directions by sensors S-1 and S-2, respectively. Then, taking into account the obtained results of the mode shapes, the natural frequencies from this paper and the bending moments and the total unit elongations from [26] can determine a mathematical model of the smart structure in the state-space form. Similarly to the previous model (the estimated model), also in this case the full model of the plate is described by two separate sub-models, called "odd modes" and "even modes", where each of them is written is the following form:

$$\begin{aligned} \dot{\mathbf{x}}(\mathrm{t}) &= \mathbf{A}\mathbf{x}(\mathrm{t}) + \mathbf{B}\varepsilon(U_s), \\ \mathbf{u}_{\mathrm{sensor}}(\mathrm{t}) &= \mathbf{C}\mathbf{x}(\mathrm{t}). \end{aligned} \tag{14}$$

In the case of the considered "odd modes" subsystem, the triplet matrices $\mathbf{A}$, $\mathbf{B}$, $\mathbf{C}$ from eq. (14) have the following form:

$$\mathbf{A} = \begin{bmatrix} 0 & 0 & 0 & 1 & 0 & 0 \\ 0 & 0 & 0 & 0 & 1 & 0 \\ 0 & 0 & 0 & 0 & 0 & 1 \\ -\omega_1^2 & 0 & 0 & -2\xi_1\omega_1 & 0 & 0 \\ 0 & -\omega_3^2 & 0 & 0 & -2\xi_3\omega_3 & 0 \\ 0 & 0 & -\omega_5^2 & 0 & 0 & -2\xi_5\omega_5 \end{bmatrix}, \quad \mathbf{B} = \begin{bmatrix} 0 \\ 0 \\ 0 \\ M_{X\_1} \\ M_{X\_3} \\ M_{X\_5} \end{bmatrix}, \quad \mathbf{C} = \begin{bmatrix} C_{X\_1} \\ C_{X\_3} \\ C_{X\_5} \\ 0 \\ 0 \\ 0 \end{bmatrix}^T,$$

where

$$\left.\begin{aligned} M_{X\_i} &= d_{31} \cdot (-z_i(x_{p1}, y) + 2z_i(x_{p2}, y) - z_i(x_{p3}, y)) + d_{32}(-z_i(x, y_{p1}) + 2z_i(x, y_{p2}) - z_i(x, y_{p3})) \\ C_{X\_i} &= -e_{31} * h_s * b_p * (-z_i(x_{p1}, y) + 2z_i(x_{p2}, y) - z_i(x_{p3}, y)) \end{aligned}\right\}, \quad \text{for } i = 1, 3, 5.$$

The obtained sub-model is transformed into the partial-fraction form, shown in eq. (15), in order to conduct the analysis of the residues.

$$\begin{aligned} G_{\mathrm{Exact\_odd}}(s) = {} & \frac{-0.1054 + 1.747j}{s - (-11 - 183.1j)} + \frac{-0.1054 - 1.474j}{s - (-11 - 183.1j)} + \frac{-0.0435 + 0.811j}{s - (-44.5 - 748.2j)} \\ & + \frac{-0.0435 - 0.0811j}{s - (-44.5 - 748.2j)} + \frac{0.0051 + 0.0832j}{s - (-16.8 + 1364.0j)} + \frac{0.0051 - 0.0832j}{s - (-16.8 + 1364.0j)} - 0.0036. \end{aligned} \tag{15}$$

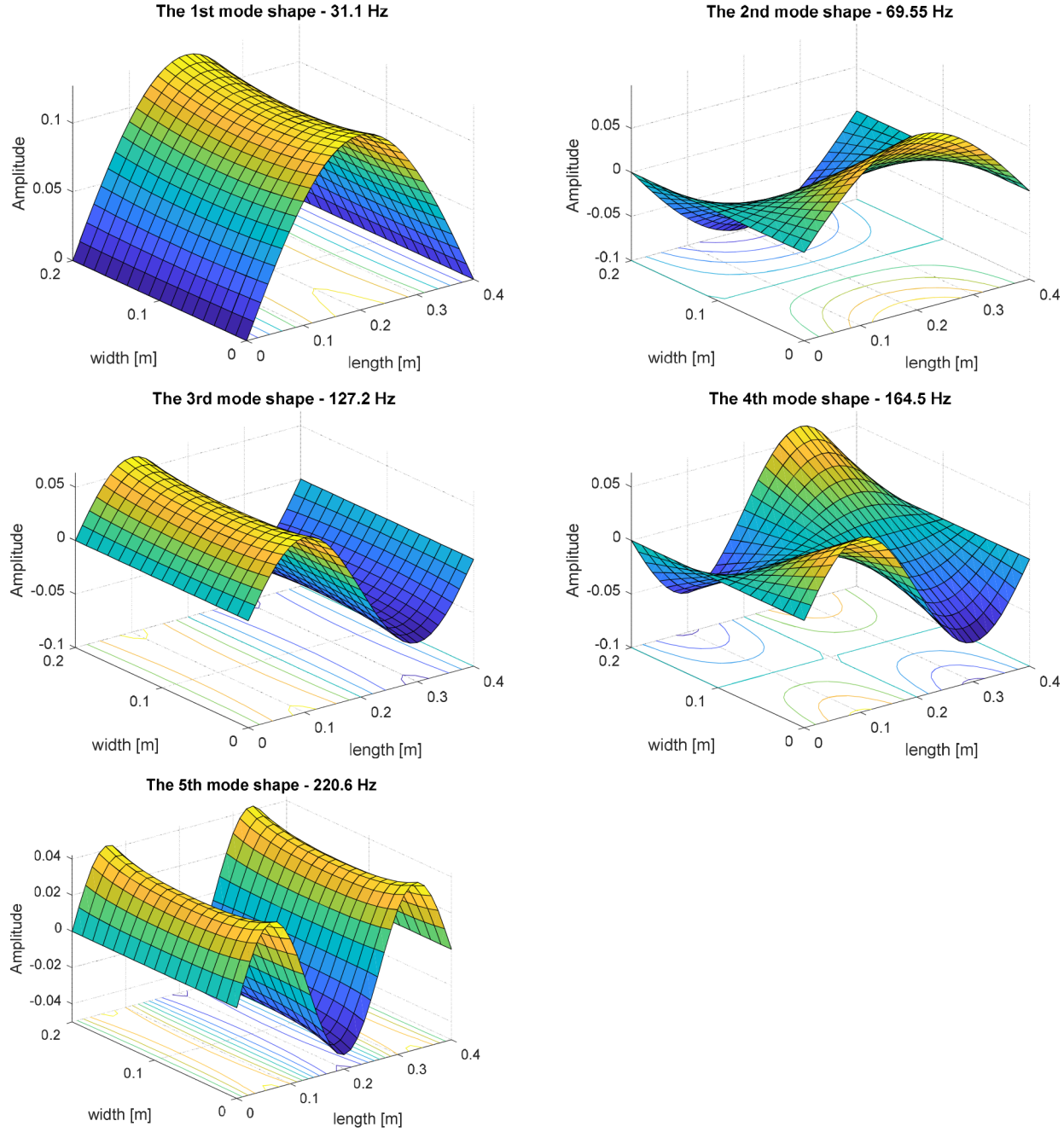

Fig. 4. The mode shapes of the SFSF smart plate in selected frequency ranges between 10–250 Hz.

Taking into account the obtained formula, we can notice that this reduction method allows obtaining the same values of the natural frequencies, as it was in the case of eq. (10), but a different value of the sum of residues −0.2877. As it can be seen, the obtained value of the residue sum is close to the value of the sum calculated for the estimated model (see eq. (10)). Thus, taking into account this result, we may suppose that also the value of the boundary gain for this model can be very close to the value of 24.28. In order to verify it, again with the help of the root-locus method, this model is investigated. As it can be seen in fig. 5(b), the obtained result confirmed the above supposition because the obtained value of 25.51 is close to the boundary gain achieved for the estimated model. This also leads to the final conclusion that the control system designed for this model is stable for the gain controller less than 25.51.

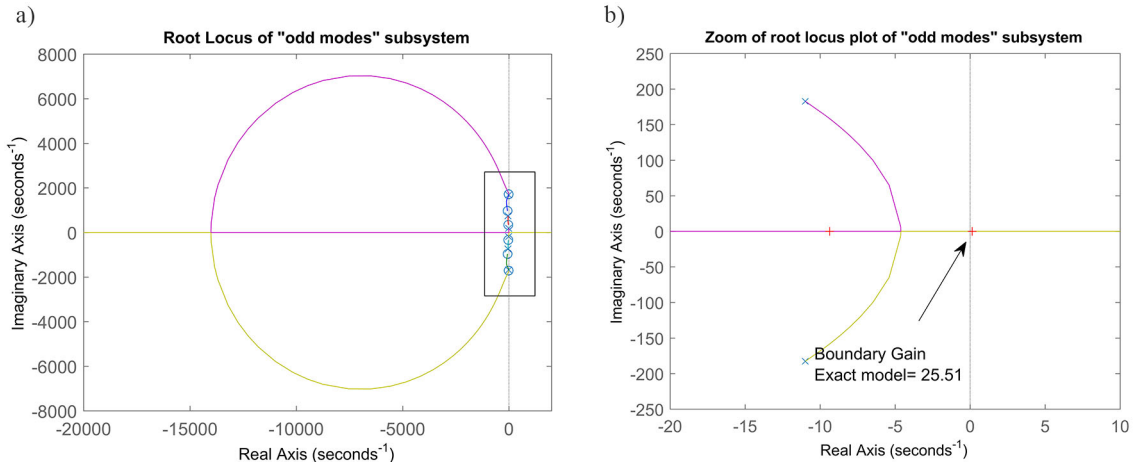

Fig. 5. The Evans plot of the reduced order model obtained from the modal analytical decomposition (a) in full range, (b) in the selected range.

Modal decomposition (numerical approach)

In this section the reduced damped model of the plate is achieved by applying the described numerical approach in the modal decomposition in ref. [26]. For this purpose, the obtained global stiffness K and the mass M matrices from the aforementioned paper allow to calculate the state matrix $\mathbf{A_m}$ in eq. (19), the Rayleigh damping matrix $\mathbf{C}$ (see eq. (16)) and determining the eigenvectors $\mathbf{V}$ and eigenvalues ϕ according to eq. (17),

$$\mathbf{C} = \alpha\mathbf{M} + \beta\mathbf{K}, \tag{16}$$

where $\mathbf{M} = \mathbf{G^T M_e G}$ is the mass matrix of the smart plate in global coordinates, $\mathbf{K} = \mathbf{G^T K_e G}$ is the stiffness matrix of the smart plate in global coordinates, $\mathbf{G}$ is the boundary matrix, α, β are the constants of proportionality,

$$(\mathbf{K} - \omega^2\mathbf{M})\mathbf{x} = \mathbf{0}, \tag{17}$$

where ω is the frequency resonance of the plate.

As was mentioned in the previous section, the plate is excited to vibration with the use of piezo-actuators which generate bending moments $Mx(x, y)$ or $My(x, y)$. As a result of such excitation, eq. (1) is modified to the following form:

$$\mathbf{M}^*\ddot{\mathbf{q}} + \mathbf{C}\dot{\mathbf{q}} + \mathbf{K}^*\mathbf{q} = \mathbf{M}^*_X + \mathbf{M}^*_Y, \tag{18}$$

where $\mathbf{M}^* = \boldsymbol{\varphi}^\mathbf{T}\mathbf{M}\boldsymbol{\varphi}$, $\mathbf{C}^* = \boldsymbol{\varphi}^\mathbf{T}\mathbf{C}\boldsymbol{\varphi}$, $\mathbf{K}^* = \boldsymbol{\varphi}^\mathbf{T}\mathbf{K}\boldsymbol{\varphi}$ are the modal matrices of mass, damping and stiffness, respectively, $\mathbf{M}^*_X = \boldsymbol{\varphi}^\mathbf{T}\mathbf{M}_X$, $\mathbf{M}^*_Y = \boldsymbol{\varphi}^\mathbf{T}\mathbf{M}_Y$ are the modal bending moments generated by the A-1 or A-2 piezos, respectively, $\mathbf{q} = \boldsymbol{\varphi}\mathbf{x}$ is the modal coordinate.

The force motion equation of the plate written in eq. (18) allows determining a model of the structure expressed in eq. (19). As it can be seen in the mentioned equation, the obtained model is described by two inputs and two outputs. Since the main goal of this paper was to design a low energy control system, the obtained model is decoupled into two SISO subsystems. As a result two sub-systems are obtained to separately control chosen modes (even or odd modes) in the frequency range of 10–250 Hz. Both sub-systems are expressed in eq. (20),

$$\begin{aligned} \dot{\mathbf{x}}(t) &= \mathbf{A_m}\mathbf{x}(t) + \mathbf{B_m}\mathbf{u}(t), \\ \mathbf{y}(t) &= \mathbf{C_m}\mathbf{x}(t), \end{aligned} \tag{19}$$

where

$$\mathbf{A_m} = \begin{bmatrix} \mathbf{0} & \mathbf{I} \\ -\mathbf{M^*}^{-1}\mathbf{K^*} & -\mathbf{M^*}^{-1}\mathbf{C^*} \end{bmatrix}_{(3298\times3298)} \quad \text{is the state matrix,}$$

$$\mathbf{B_m} = \begin{bmatrix} \mathbf{B}_X & \mathbf{B}_Y \end{bmatrix} = \begin{bmatrix} \mathbf{0} & \mathbf{0} \\ \mathbf{M^*}^{-1}\boldsymbol{\varphi}^\mathbf{T}\mathbf{M}_X(x,y) & \mathbf{M^*}^{-1}\boldsymbol{\varphi}^\mathbf{T}\mathbf{M}_Y(x,y) \end{bmatrix}_{(3298\times2)} \quad \text{is the input matrix,}$$

$$\mathbf{C_m} = \begin{bmatrix} \mathbf{C}_X \\ \mathbf{C}_Y \end{bmatrix} = \begin{bmatrix} 0 & (e_{31} * b_s * h_s) \cdot \mathbf{S}_X \cdot \boldsymbol{\varphi} \\ 0 & (e_{31} * b_s * h_s) \cdot \mathbf{S}_Y \cdot \boldsymbol{\varphi} \end{bmatrix}_{(2\times3298)} \quad \text{is the output matrix;}$$

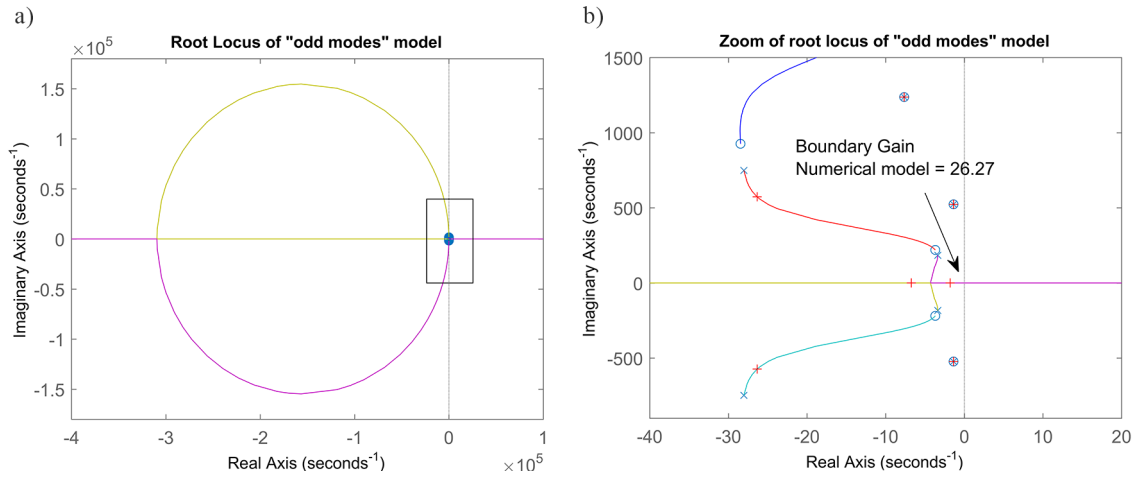

Fig. 6. The Evans plot of the "odd modes" models obtained by using the numerical approach: (a) in full gain range; (b) in the selected gain range.

$$\begin{aligned} &\textit{"odd modes" subsystem} && \textit{"even modes" subsystem} \\ &\dot{\mathbf{x}}_{\text{odd}}(t) = \mathbf{A}_{\text{odd}}\mathbf{x}(t) + \mathbf{B}_{\text{odd}}\mathbf{u}(t), && \dot{\mathbf{x}}_{\text{even}}(t) = \mathbf{A}_{\text{even}}\mathbf{x}(t) + \mathbf{B}_{\text{even}}\mathbf{u}(t), \\ &\mathbf{y}_{\text{odd}}(t) = \mathbf{C}_{\text{odd}}\mathbf{x}(t); && \mathbf{y}_{\text{even}}(t) = \mathbf{C}_{\text{even}}\mathbf{x}(t), \end{aligned} \tag{20}$$

where $\mathbf{A}_{\text{odd}} = \begin{bmatrix} \mathbf{0} & \mathbf{I} \\ -\mathbf{M}^{*^{-1}}\mathbf{K}^* & -\mathbf{M}^{*^{-1}}\mathbf{C}^* \end{bmatrix}$, $\mathbf{B}_{\text{odd}} = [\mathbf{B}_X] = \begin{bmatrix} 0 \\ \mathbf{M}^{*^{-1}}\boldsymbol{\varphi}^{\mathbf{T}}\mathbf{M}_{X(x,y)} \end{bmatrix}$, $\mathbf{C}_{\text{odd}} = [\mathbf{C}_X] = \begin{bmatrix} 0 & (e_{31} * b_s * h_s) \cdot \mathbf{S}_X \cdot \boldsymbol{\varphi} \end{bmatrix}$, $\mathbf{S}_X = (-\mathbf{V}(x_{p1}, y) + 2\mathbf{V}(x_{p2}, y) - \mathbf{V}(x_{p3}, y))$; $\mathbf{A}_{\text{even}} = \begin{bmatrix} \mathbf{0} & \mathbf{I} \\ -\mathbf{M}^{*^{-1}}\mathbf{K}^* & -\mathbf{M}^{*^{-1}}\mathbf{C}^* \end{bmatrix}$, $\mathbf{B}_{\text{even}} = [\mathbf{B}_Y] = \begin{bmatrix} 0 \\ \mathbf{M}^{*^{-1}}\boldsymbol{\varphi}^{\mathbf{T}}\mathbf{M}_{Y(x,y)} \end{bmatrix}$, $\mathbf{C}_{\text{even}} = [\mathbf{C}_Y] = \begin{bmatrix} 0 & (e_{31} * b_s * h_s) \cdot \mathbf{S}_Y \cdot \boldsymbol{\varphi} \end{bmatrix}$, $\mathbf{S}_Y = ((-\mathbf{V}(x, y_{p1}) + 2w\mathbf{V}x, y_{p2}) - \mathbf{V}(x, y_{p3}))$.

The determined models, similar as in the previous sections, are transformed to the partial-fraction form. The result of this transformation for "odd model" is a model achieved as follows:

$$\begin{aligned} G_{\text{Modal\_Numerical\_Odd}}(s) = &\frac{-0.0019 + 1.0703j}{s - (-3.4 - 183.7j)} + \frac{-0.0019 - 1.0703j}{s - (-3.4 + 183.7j)} + \frac{-0.0134 + 3.4019j}{s - (-28 - 748.1j)} \\ &+ \frac{-0.0134 - 3.4019j}{s - (-28 - 748.1j)} + \frac{-0.0071 + 0.417j}{s - (-14.6 - 1362.1j)} + \frac{-0.0071 + 0.417j}{s - (-14.6 - 1362.1j)} - 0.0168. \end{aligned} \tag{21}$$

Taking into account all residues of the model in eq. (21), we can notice that their sum equals -0.0616. The value obtained in this way diverges from the result calculated for the estimated model (-0.4308). Thus, it can be expected that also the value of the boundary gain calculated for this model will be distant from the value of 24.28. As it is shown in fig. 6(b), the above supposition is confirmed because the boundary gain for this model should not exceed 26.27.

Schur decomposition

The Schur decomposition is the last orthogonal method considered in the paper. For this purpose, the state space matrix of the "odd modes" damped model from eq. (20) is decomposed to an orthogonal matrix $\mathbf{U}$ which represents mode shapes and an upper triangular matrix $\mathbf{T}$. As a result of such decomposition, the order of the model is reduced and expressed in the partial-fraction form again (see eq. (23)), according to

$$\mathbf{U} \cdot \mathbf{T} \cdot \mathbf{U}^{\mathbf{T}} = \mathbf{A}_{\text{odd}}, \tag{22}$$

where $\mathbf{A}_{\text{odd}} = \begin{bmatrix} \mathbf{0} & \mathbf{I} \\ -\mathbf{M}^{*^{-1}}\mathbf{K}^* & -\mathbf{M}^{*^{-1}}\mathbf{C}^* \end{bmatrix}$.

$$\begin{aligned} G_{\text{Schur\_odd}}(s) = &\frac{-0.0007 + 0.1508j}{s - (-8.8 - 183.5j)} + \frac{-0.0007 - 0.1508j}{s - (-8.8 + 183.5j)} + \frac{-0.0002 + 0.2018j}{s - (-24.5 - 748.2j)} \\ &+ \frac{-0.0002 - 0.2018j}{s - (-24.5 - 748.2j)} + \frac{-0.0022 + 2.6082j}{s - (-21.9 - 1364j)} + \frac{-0.0022 - 2.6082j}{s - (-21.9 - 1364j)} - 0.0061. \end{aligned} \tag{23}$$

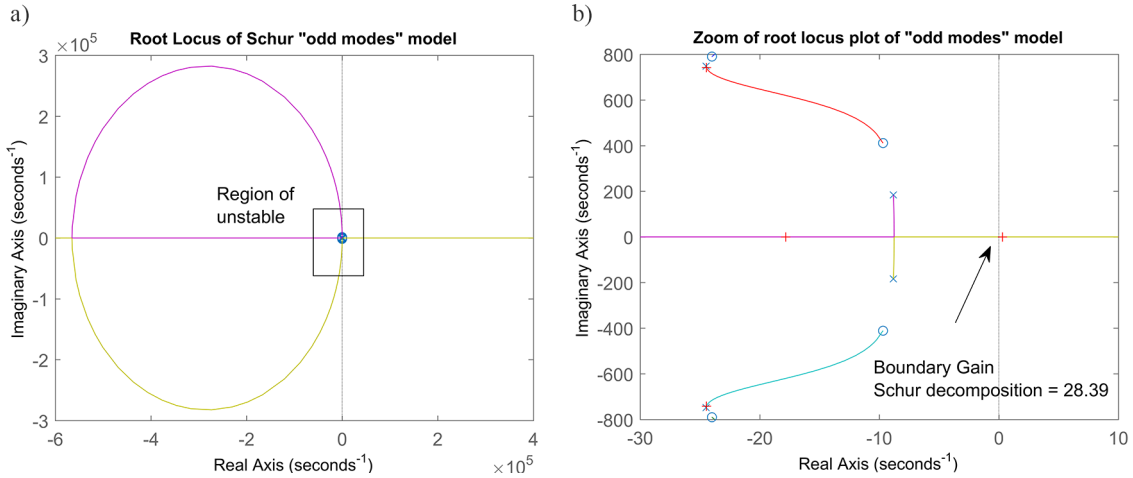

Fig. 7. The Evans plot of the reduced order of the "odd modes" model obtained from Schur decomposition.

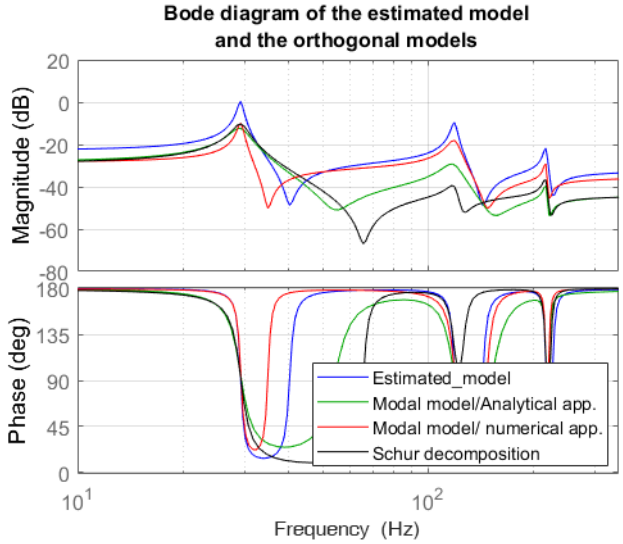

Fig. 8. Bode plots of orthogonal models: Ritz, Schur, modal numerical and modal analytical (exact solution) in the range of the first three lowest natural frequencies.

Again, as it was observed in previous models, the value of the residue sum is calculated and root-locus curves for this model are plotted. The result of the analysis of the residues values showed that the sum of the residues equals -0.0063 and it is the worst result in comparison to previous results. A similar result is achieved in the case of determining a boundary gain with the help of the Evans plot (see fig. 7). Then, in this case, the determined gain is 28.39 and it is also the worst result. From the control point of view of this structure, such divergence between the obtained results and the results obtained for the estimated model may lead to instability of the designed control system during experimental tests.

Comparison of orthogonal methods

The dynamic parameters of all orthogonal methods considered in the previous sections are collected in table 2. Taking into account this table and the Bode plot shown in fig. 8, it can be noticed that all orthogonal methods (modal analytical, modal numerical and Schur decomposition) generate the same value of the first three odd natural frequencies but calculate different anti-resonances frequencies. Additionally, analyzing the phase plot of these models, we can see proper interlacing between poles and zeros, which is a typical feature of collocated systems and a desirable effect of some non-collocated systems. From the strategy control point of view, it is especially important because zeros of particular models are represented by anti-resonance frequencies and have a direct influence on the control law designing procedure. Thus, in order to stabilize the closed-loop system for different models, the root-locus plots with

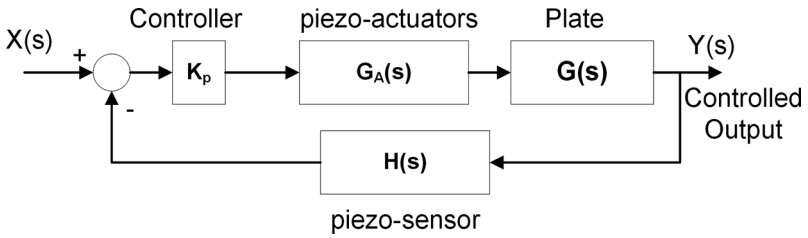

Fig. 9. The control system of the smart plate.

Table 2. Values of the natural frequencies, anti-resonance frequencies and feedback gains for different orthogonal methods and the recorded data.

Orthogonal method/ Experimental results	1st mode frequency [Hz]		3rd mode frequency [Hz]		5th mode frequency [Hz]		Boundary gain
	resonance	anti-resonance	resonance	anti-resonance	resonance	anti-resonance	k_{kr}
Estimated model	29.2	40.3	119.1	143	217.0	272.0	24.28
Modal/analytical	29.2	53.9	119.1	157	217.2	221.6	25.51
Modal/numerical	29.2	34.9	119.1	147	216.9	221.4	26.27
Schur	29.2	65.4	119.1	128	217.2	223.7	28.27
Measurement	30.0	37.9	124.5	128.5	216.4	246.6	–

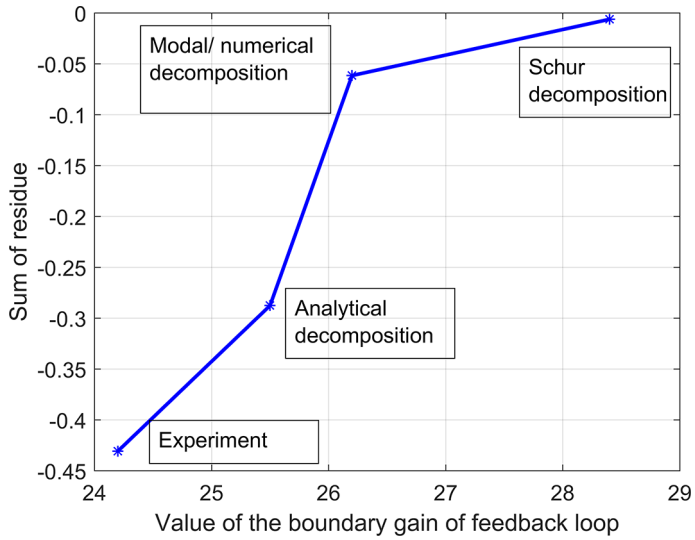

Fig. 10. Comparison of sums of residues of the orthogonal methods related to the "odd modes" model *versus* the boundary gain of the feedback loop.

different values of boundary gains in the feedback loop are obtained. Taking into account the considered orthogonal methods and the structure of the closed-loop system shown in fig. 9, we can notice that the best boundary gain is obtained for the analytical modal model. In this case, the control system is very close to the closed-loop system with an estimated model determined in an identification process. On the other hand, the worst results are achieved for the Schur decomposition where the value of the feedback loop gain is the farthest away from the value of 24.28, achieved for the estimated model.

Next, the sum of the residue values of particular damped "odd modes" models was calculated. As it can be seen in fig. 10, there exists a strong correlation between the sum of residues of each reduced model and the boundary value of the feedback gain. Again the best solution is obtained for the exact solution, but the worst result —for the Schur decomposition. In this case the sum of residue for the exact model is the nearest value of the achieved for the estimated model and the value of the boundary gain is close to the feedback gain determined for the estimated model. On the other hand, the worst result was obtained for the Schur decomposition. In this case, both values of the sum of residues and the boundary gain are far from the $(-0.4308; 24.28)$ results, respectively.

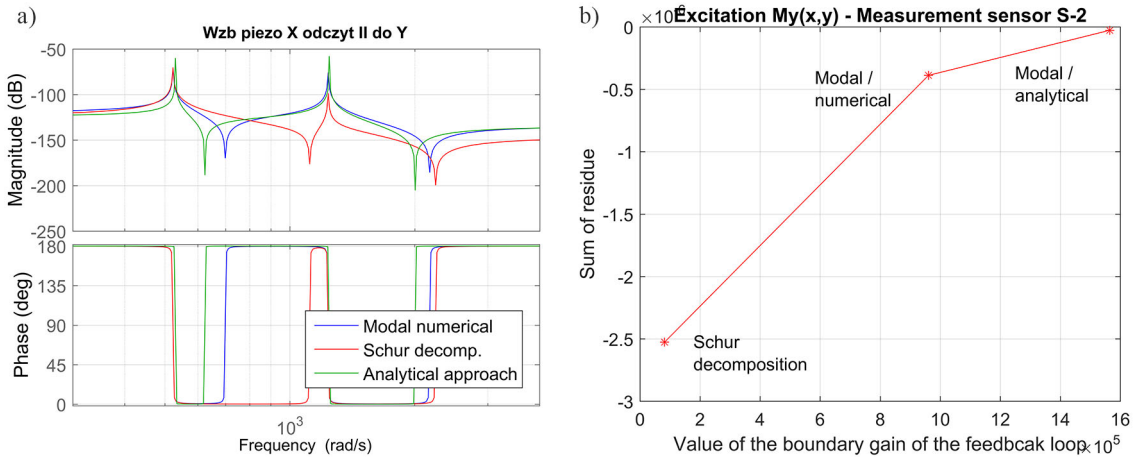

Fig. 11. (a) The Bode plot of orthogonal models determined for the "even model" subsystem. (b) Comparison of sums of residues of the orthogonal methods related to the "even modes" subsystem *versus* the boundary gain of the feedback loop.

Analysis of orthogonal methods in the case of lightly damped models

The dynamic parameters of all orthogonal methods were also investigated for the second subsystem called "even modes", but in this case these systems represent lightly damped models. Just to remind in order to obtain this sub-model, the considered plate is excited to vibration by the bending moment $My(x, y)$, while the vibration amplitude is measured by the S-2 sensor oriented longitudinally to the vertical axis of the plate. Similarly to the "odd modes" subsystem, the reduced order models are determined and compared. For each of them the sum of residues of the open-loop subsystem and the value of the boundary gain are determined with the use of the root-locus method. Apart from this, also the amplitude plot for each model is plotted. All the obtained results are shown in fig. 11.

Taking into account the amplitude plot shown in fig. 11(a), we can notice that also in this case all orthogonal methods (modal analytical, modal numerical and Schur decomposition) generate the same value of the first two even natural frequencies but calculate different anti-resonances frequencies. Again, the behavior of interlacing the poles and zeros of each model is saved. On the other hand, taking into account fig. 11(b), it can be seen that in this case all calculated values of the sum of residue should be convergent to zero. Thus, analyzing this plot, we can notice that the best boundary gain is obtained once again for the analytical modal model, but the worst for the Schur decomposition. As a result, the analytical model ensures the stability of the control system in the highest range of the gain change of the controller, but in the case of the Schur model —in the narrowest range.

Experimental investigations

In this section, the behavior of decomposition methods is assessed on the basis of experimental set-up carried out only for the estimated model. For this purpose, as the first step, the designed control law for a chosen model was implemented to the Dspace controller by an inbuilt to the Matlab/Simulink software toolbox. During experimental investigations, the chirp signal with the frequency within the range of 10–250 Hz is chosen again as the excitation signal. The generated signal, according to fig. 12, was added to the control signal $u(t)$ and then applied to the piezo-actuator A-1 by a D/A card located on the DSP controller board. As a result, the bending moment $Mx(x, y)$ was generated and this leads to its vibrations measured by the piezoelectric sensor S-1. The amplitude plot of the closed-loop system obtained as a result of the experiment was recorded by the Digital Signal Analyzer and shown in fig. 13(b).

As it can be seen in fig. 13(b), the amplitude plot of the control system obtained during the test-rig is a good fitting to the amplitude plot of the feedback system from simulations. It is especially visible near the first two peaks of odd natural frequencies, where the values of the amplitude vibrations are similar. An additional analysis of these plots showed that also some additional damp in the control system appeared. As a result, the amplitude of vibrations of the experimental control system was reduced of about 4 dB *versus* the amplitude of the open-loop system. Again, the most visible effect of such reduction of amplitude was achieved by the first natural frequency. The comparison of frequencies that lead the system to the boundary stability confirms that the control law has been properly designed. In both cases the aforementioned frequency is the same and equals 19.7 Hz.

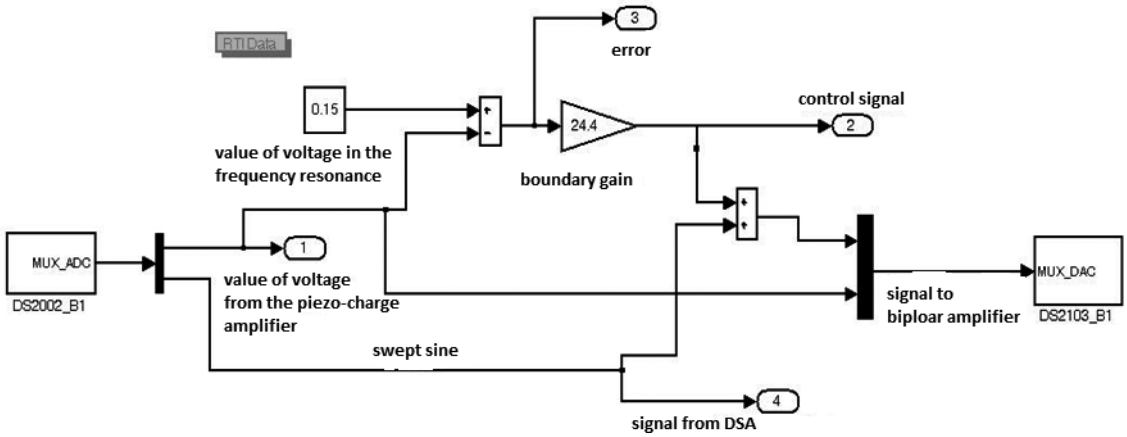

Fig. 12. The control system designed in Simulink software with A/D and D/A cards of Dspace controller.

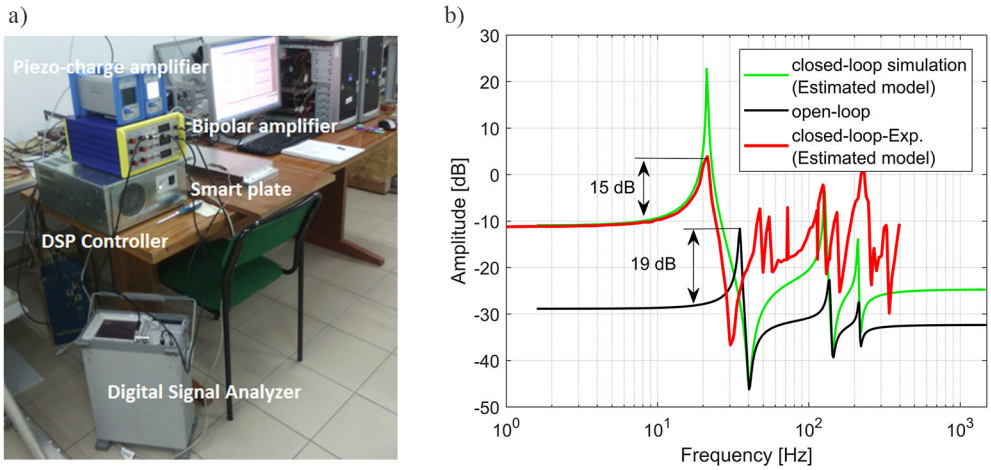

Fig. 13. (a) Photo of the laboratory stand during an experimental test of the designed control system. (b) Amplitude plots of the open-loop "odd modes" system and control systems (simulation and experiment) within the frequency range of 1–1000 Hz.

Summary

The real flexible structures are described by a mathematical model of multi-degree freedom. For an active vibration control system, the model of the considered mechanical structure should be reduced to a few degrees of freedom. For this reason, the process of reduction of the order model is a very crucial step and should be analyzed carefully in accordance with a real closed-loop system. An SFSF plate with piezo-stripes, (actuator/sensor) located on the top and bottom surfaces in their quasi-optimal placements, was the mechanical structure analyzed in this paper. In the results of such distributions of piezo-elements on the structure, two non-collocated control systems are determined and each of them allows controlling the chosen modes of the plate (odd or even modes). For such a decoupled system, the estimated models called "odd modes" and "even modes", were estimated with the use of an identification procedure. Then, the model called "odd modes" was described by three lowest odd frequencies (resonance and anti-resonance), but the "even modes" model —by only the first two lowest even frequencies (resonance and anti-resonance). The obtained models are transformed to the partial-fraction form model, where the calculated sum of residues of a particular model became an indicator to determine the boundary gain of the feedback loop with the use of the root-locus method. A similar decomposition procedure was repeated to determine the reduced order models by using orthogonal methods like: modal analytical approach, modal numerical approach and Schur decomposition. Then, the obtained results presented in figs. 10 and 11(b) for strongly and lightly damped models showed that in both cases the best results are achieved for the analytical model, while the worst —for the Schur model. Taking into account the analytical model, the calculated value of the sum of residues (-0.2877) is closest to the calculated value for the estimated model (-0.4308), or it is closest to the zero in the case of the lightly damped model. As a result, the control system is only stable in the vicinity of the feedback gain calculated for the estimated model ($k_{kr} = 24.28$); or in the case of the lightly damped "even modes models, it is stable in the highest range of the feedback gain.

Further analysis of the influence of the orthogonal methods on the control system was carried out in the frequency domain. The obtained Bode characteristics for both considered kinds of SISO models ("odd modes", strongly damped, and "even modes", lightly damped) presented in fig. 8 and fig. 11(a) indicated that each of the considered orthogonal method properly calculates natural frequencies but generates different anti-resonance frequencies. As a result, this leads to obtain a different value of boundary gains in the feedback loop.

The obtained simulations results for strongly damped model are tested on the lab stand. For this purpose, the designed control law for only the estimated model is implemented to a DSP controller by Matlab/Simulink software. This leads to confirm the previously assumed supposition that the best orthogonal method is the analytical decomposition, because the value of the experimental boundary gain ($k_{kr} = 24.4$) is close to the values determined for the estimated model ($k_{kr} = 24.28$) and the analytical model ($k_{kr} = 25.51$). Additionally, the analysis of the experimental amplitude plot of the control system showed that the estimated model was properly determined because the boundary frequency of the control system experimental testing ($f_{\text{bound}} = 19.7\,\text{Hz}$) is the same as in the case of simulations (see fig. 3).

Conclusions

The proposed method, referring to the residue analysis of the model, allows designing an active vibration control for a structure with an actuator and a sensor located very close to each other (the sensor behind the actuator). The modal analysis carried out for the considered structure leads to decoupling the MIMO system into SISO-subsystems and designing the control law for each of them by using the root-locus method. The obtained modal values of the piezo-actuator and the piezo-sensor displacements in the chosen frequency range allowed to calculate residues for the considered modes and then design the control law, based on the obtained values of residues. The decomposition of the obtained SISO sub-models, additionally carried out in the paper, showed that different values of residues for each orthogonal method may be obtained. As a result, it has been indicated that the calculated sum of residues can be an indicator of choosing the best decomposition method while designing an active vibration control system, especially for this kind of smart structures.

Taking into account 1D or 2D structures, it is known that the exact model can be obtained by using the analytical approach. Then, the designed control law for this model, based on the proposed method, should also be most convergent to the control law designed for the estimated model. However, as is known, nowadays, structures are more complicated. Then, in order to simplify the process of designing the control law by using the residue analysis, the numerical model should be used. As a result, the obtained modal parameters of the model with considered modal displacements of a piezo-sensor and a piezo-actuator for chosen modes should allow determining a partial fraction form the model, calculate the sum of residues and design the control law.

Finally, it can be noted that the proposed method combined with the root-locus method can be especially useful for structures whose models may be decoupled into SISO sub-systems.

This work is supported with *University Work* no. S/WM/1/2016 of the Department of Automatic Control and Robotics, Bialystok University of Technology.

References

1. W. Gawroński, K.B. Lim, *Balanced Control of Flexible Structures* (Springer, London,1996).
2. M.J. Balas, IEEE Trans. Autom. Control **23**, 4 (1978).
3. E.H. Maslen, G. Schweitzer, *Magnetic Bearings Theory, Design and Application to Rotating Machinery* (Springer Publisher, Dordrecht Heidelberg London, 2009).
4. N. Chailet, M. Grossard, S. Regnier, *Flexible Robotics, Applications to Multiscale Manipulators* (ISTE Ltd., London, John Wiley & Sons, Hoboken, 2013).
5. Z. Kulesza, J. Vib. Control **21**, 8 (2015).
6. A. Preumont, *Vibration Control of Active Structures, An Introduction*, second edition (Kluwer Academic Publisher, Dordrecht, 2002).
7. M.S. Tombs, I. Postlethwaite, Int. J. Control **46**, 1319 (1987).
8. J.N. Juang, *Applied System Identification* (Prentice Hall, Inc. UK, 1994).
9. Z. Osiński, *Theory of Vibrations* (PWN Press, Warsaw, 1990) (in Polish).

10. Z. Gosiewski, Z. Kulesza, in *Proceedings of 14th International Carpathian Control Conference, 2013* (Poland, Rytro, 2013).
11. A. Mystkowski, A. Koszewnik, Mech. Syst. Signal Process. **78**, 18 (2016).
12. L. Meirovitch, H. Oz, J. Guid. Control **3**, 3 (1980).
13. L. Meirovitch, H. Oz, H.F. Van Landingham, J. Guid. Control **2**, 5 (1979).
14. Z. Gosiewski, A. Koszewnik, J. Vibroeng. **14**, 2 (2012).
15. Z. Gosiewski, A. Koszewnik, Solid State Phenom. **144**, 59 (2007).
16. A. Quarteroni, R. Sacco, F. Saleri, *Numerical Mathematics, Approximation of Eigenvalues and Eigenvectors, Part II* (Springer, New York, 2007).
17. S.G. Kelly, *Advanced Vibration Analysis* (CRC Press, Taylor & Francis Group, 2007).
18. B. Sapiński, Smart Mater. Struct. **20**, 105007 (2011).
19. Z. Gosiewski, A. Mystkowski, Mech. Syst. Signal Process. **22**, 66 (2013).
20. Z. Gosiewski, A. Koszewnik, Mech. Syst. Signal Process. **36**, 136 (2013) Special Issue of Piezoelectric Technology.
21. J. Konieczny, J. Kowal, B. Sapiński, *Proceedings of the International Symposium on Active Control of Sound and Vibration*, Vols. **1** & **2** (Florida, USA, 1999).
22. G.L. Anderson, H.S. Tzou, *Intelligent Structural Systems* (Kluwer Academic Publishers, 1992).
23. J.J. Hollkamp, H.S. Tzou, J.P. Zhong, J. Sound Vib. **177**, 3 (1994).
24. Z. Gosiewski, J. Theor. Appl. Mech. **46**, 4 (2008).
25. A. Koszewnik, Z. Gosiewski, Solid State Phenom. **248**, 119 (2016).
26. A. Koszewnik, Z. Gosiewski, Eur. Phys. J. Plus **131**, 232 (2016).
27. A. Preumont, *Twelve Lectures on Structural Dynamics* (Springer, New York, 2013).
28. A.J.M. Ferreira, *Matlab Code for Finite Element Analysis: Solids and Structures* (Springer Publisher, 2009).